Uniform Spinning Sampling Gradient Electron Paramagnetic Resonance Imaging

David H Johnson[1], Zhiyu Chen[1], Rizwan Ahmad[1], Alexandre Samouilov[1], and Jay L Zweier[1]
[1]*Davis Heart and Lung Research Institute, Ohio State University, Columbus, OH, United States*

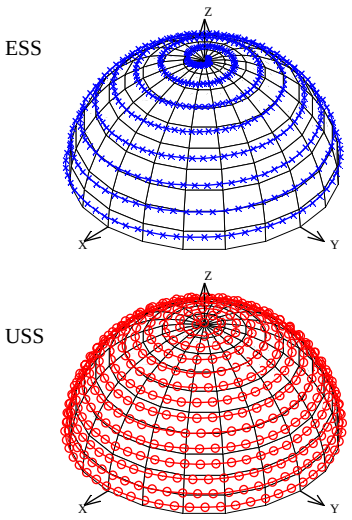

Figure 1. Comparison of sampling strategies for N=400 projections

Target Audience. This work will benefit Electron Paramagnetic Resonance (EPR) researchers and cardiologists interested in studying oxygen levels in vivo using rapid imaging techniques.

Purpose. This research was performed to improve the efficiency of the EPR spinning gradient acquisition to produce better images of the isolated rat heart model of ischemic heart disease. The well-known limitation of oversampling the Z axis in the traditional spinning gradient acquisition results in an inefficient allocation of acquisition time and thus suboptimal images[1]. By fixing this problem, the spinning gradient acquisition provides fast, high quality images of the rat heart, which will enable future studies of noninvasive measurement of changes in oxygen during the cardiac cycle.

Methods. The Uniform Spinning Sampling (USS) distribution was derived for N projections on the unit hemisphere by applying an arcsin transformation[2] to the polar angle (φ) and rescaling the azimuth angle (θ) according to the following formulas: $\varphi=\arcsin((t-1)/(N-1))$ and $\theta=\varphi\sqrt{(2\pi N)}$ where t is [1,2,…N]. In comparison, the traditional Equilinear Spinning Sampling (ESS) distribution is defined as $\varphi=\pi(t-1)/(2N-2)$ and $\theta=-4R(\pi/2-\varphi)$ where R is a free parameter determined by the relative rates at which the X-Y component of the gradient vector rotates with respect to the Z component. R=8 was used in previous work[1] and in this study. The gradient vector was defined as $Gx=\cos(\varphi)\cos(\theta)$, $Gy=\cos(\varphi)\sin(\theta)$, and $Gz=\cos(\theta)$. ESS has approximately twice as many projections near the Z pole as near either the X or Y axes (Fig 1, top). In contrast, USS places an equal number of projections near all three axes (Fig 1, bottom).

The two acquisition strategies were simulated in reconstructing a 3D Shepp-Logan phantom. N=1,024 noiseless projections were simulated along either the angles specified by USS or by ESS, and then images were reconstructed by filtered backprojection on a 128x128x128 grid.

An EPR experiment was conducted on a 1.2 GHz CW system with the isolated rat heart model of ischemic heart disease. Surgery was performed on an adult rat under anesthesia to extract the heart, which was then perfused with PBS, calcium, and 20 mg/ml Lithium Phthalocyanine (LiPc) through the cannulated aeorta. The heart was maintained in cardioplegia with a balloon in the left ventricle (LV) while EPR projections were acquired using the USS and then ESS acquisition strategies (N=1,024 projections in 4.5 min for each acquisition). Images were reconstructed using standard EPR corrections[3] followed by filtered backprojection in Matlab. Signal to noise ratio (SNR) was measured in the reconstructed images by dividing the maximum signal intensity in the image by the standard deviation of the non-signal regions of the image. The USS images were then visualized in 3D using isosurface renderings with contours set to the outer myocardial wall, the right ventricle (RV), and the balloon.

Results. The Shepp-Logan phantom reconstruction showed a lack of resolution in the X-Y plane when ESS was used (Fig 2-a) whereas USS produced improved resolution along all axes (2-b). Radial streaking artifacts were obvious in the cardiac data when ESS was used (3-a) but not for USS (3-b). SNR in the ESS image was 56.2, whereas SNR in the USS image was 85.9. Isosurface renderings of the USS images showed LiPc enhancement in the RV and a signal void in the LV (4-a and b).

Discussion. The 4.5 min USS acquisition yielded good EPR images with higher signal to noise ratio and lower radial artifacts as compared to ESS acquisitions (also 4.5 min). The problem of oversampling the Z axis is mitigated, and every projection contributes new and useful information to the reconstructed image. By repeating the USS acquisition at higher gradient amplitudes the linewidth (1/T2*) of LiPc can be measured, which provides a direct measurement of tissue oxygen.

Conclusion. EPR imaging is closer than ever before to the realization of fast, high quality cardiac acquisitions. Future research will extend USS to 4D EPR spectral-spatial imaging with more projections at higher gradient amplitudes. By adding ECG gating to the acquisition, it will be possible to dynamically measure oxygen during the cardiac cycle throughout the heart, which will enable studies of coronary occlusion and myocardial reperfusion.

References. [1] Deng et al. Fast 3D spatial EPR imaging using spiral magnetic field gradient. J Magn Reson 2007;185(2):283-290. [2] Wong STS, Roos MS. A strategy for sampling on a sphere applied to 3D selective RF pulse design. MRM 1994;32(6):778-784. [3] Eaton et al. EPR imaging and in vivo EPR. Boca Raton: CRC Press; 1991. This work was supported by NIH R01 EB004900, and the first author was supported by NIH F32 EB012932.

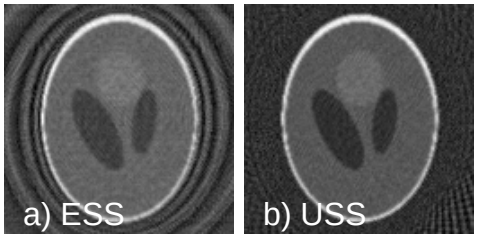

Figure 2. 3D Shepp-Logan phantom simulations demonstrate the benefits of USS over ESS. Fewer artifacts are visible in the USS image.

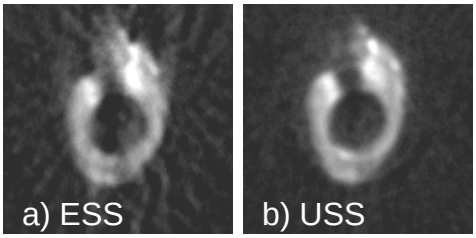

Figure 3. Isolated, ischemic heart images from ESS and USS show a signal void in the balloon and signal enhancement in the coronary sinuses and the Right Ventricle (RV).

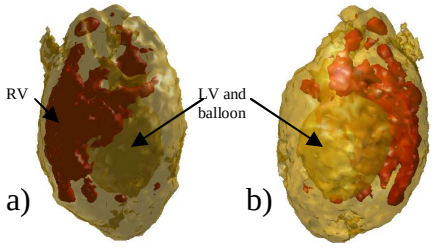

Figure 4. 3D isosurface renderings at two angles of the USS heart images display the signal void in the left ventricle (LV), which is dilated by a balloon. Enhancement in the RV is shown in red.